Imaging the Distribution of Framework Aluminum in Mesoporous Molecular Sieve MCM-41

Ryong Ryoo,*[,†,§] Chang Hyun Ko,[‡] and Russell F. Howe[†]

School of Chemistry, University of New South Wales, Sydney 2052, Australia, and Department of Chemistry and Center for Molecular Science, Korea Advanced Institute of Science and Technology, Taejon, 305-701, Korea

Received January 3, 1997. Revised Manuscript Received April 15, 1997[⊗]

The distribution of framework aluminum inside micrometer-size particles of the mesoporous molecular sieve MCM-41 has been investigated using transmission electron microscopic (TEM) images, after supporting platinum clusters inside the aluminum-containing region selectively via the ion exchange of $Pt(NH_3)_4^{2+}$. The TEM images show that the framework aluminum becomes distributed homogeneously inside the resultant MCM-41 particles if sodium aluminate is added to the reaction mixture, consisting of an aqueous solution of hexadecyltrimethylammonium (HTA) chloride and sodium silicate, before the formation of the surfactant−silicate mesostructure. On the other hand, the framework aluminum can be incorporated into the outer region within MCM-41 particles if the aluminum source is added after completing the formation of the mesostructure. The thickness of the aluminum-containing region, which results from the aluminum diffusion into the surfactant−silicate mesostructure, can be controlled by the diffusion time and the concentration of the aluminum source. In addition, powder X-ray diffraction indicates that the structural order is improved when the aluminum source is added after the formation of the surfactant−silicate mesostructure, rather than before.

Introduction

The discovery of the mesoporous molecular sieve, designated MCM-41 by researchers at Mobil Corp. in 1992, has opened a new class of molecular sieves exhibiting ordered arrangement of large pores with uniform cross-sectional diameter in the range 2−10 nm.[1,2] In addition to the remarkable increase in the pore diameter compared with zeolites, the mesoporous molecular sieves have another novelty of controlling the pore diameter over the 2−10 nm range. The control of the pore diameter is readily achieved by using surfactants with different molecular sizes and auxilliary organic species during the synthesis process,[2] and suitable postsynthetic hydrothermal treatments.[3] The uniformity and controllability of the large pore diameter has opened new possibilities for shape-selective catalytic conversion of large substrates, incorporating bulky complexes for enantioselective catalytic reactions, and templating nanosize architectures.[4]

The MCM-41 materials constructed with pure-silica framework are of limited use for various applications such as catalysis and metal incorporation, due to lack of ion-exchange capacity and acidity. The ion-exchange capacity and acidity can be produced by incorporating aluminum into the framework with various sources of aluminum.[5] Magic angle spinning (MAS) ^{27}Al NMR spectra can be used to determine the relative amounts of tetrahedral and octahedral alumina depending on the incorporating methods. In addition to the quantitative analysis, it is important to probe the spatial distribution of the framework aluminum inside the micron-sized MCM-41 particles for rational design of various materials such as catalysts based on the MCM-41. However, there have been no previous reports on the spatial distribution of the framework aluminum inside the micron-size MCM-41 particles.

In view of the spatial distribution of framework aluminum sites inside the micron-size MCM-41 particles, we have developed an imaging technique using transmission electron microscopy (TEM) after supporting platinum selectively inside the aluminum-containing region. The selective incorporation of platinum has been performed using the ion exchange of $Pt(NH_3)_4^{2+}$. The ion exchange on silica framework is negligible compared with that on the tetrahedral framework aluminum sites in MCM-41. The selective incorporation of the electron-opaque heavy metal gives rise to dark image contrast in TEM against the relatively more transparent aluminosilicate background. The imaging technique has been used to investigate the diffusion of aluminum into the surfactant−silicate mesostructures

[†] University of New South Wales.

[‡] Korea Advanced Institute of Science and Technology.

[§] On sabbatical leave from Department of Chemistry, Korea Advanced Institute of Science and Technology.

[⊗] Abstract published in *Advance ACS Abstracts,* June 1, 1997.

(1) Kresge, C. T.; Leonowicz, M. E.; Roth, W. J.; Vartuli, J. C.; Beck, J. S. *Nature* **1992**, *359*, 710.

(2) Beck, J. S.; Vartuli, J. C.; Roth, W. J.; Leonowicz, M. E.; Kresge, C. T.; Schmitt, K. D.; Chu, C. T.-W.; Olson, D. H.; Sheppard, E. W.; McCullen, S. B.; Higgins, J. B.; Schlenker, J. L. *J. Am. Chem. Soc.* **1992**, *114*, 10834.

(3) Huo, Q.; Margolese, D. I.; Stucky, G. D. *Chem. Mater.* **1996**, *8*, 1147.

(4) See, for example, a review article: Sayari, A. In *Recent Advances and New Horizons in Zeolite Science and Technology*; Chon, H., Woo, S. I., Park, S.-E., Eds.; Elsevier: Amsterdam, 1996; *Studies in Surface Science and Catalysis*; Vol. 102, p 1.

(5) See for examples: (a) Chen, C.-Y.; Li, H.-X.; Davis, M. E. *Microporous Mater.* **1993**, *2*, 17. (b) Schmidt, R.; Akporiaye, D.; Stöcker, M.; Ellestad, O. H. *J. Chem. Soc., Chem. Commun.* **1994**, 1493. (c) Corma, A.; Fornés, V.; Navarro, M. T.; Pérez-Pariente, J. *J. Catal.* **1994**, *148*, 569. (d) Luan, Z.; Cheng, C.-F.; Zhou, W.; Klinowski, J. *J. Phys. Chem.* **1995**, *99*, 1018. (e) Hamdan, H.; Endud, S.; He, H.; Muhid, M. N. M.; Klinowski, J. *J. Chem. Soc., Faraday Trans.* **1996**, *92*, 2311.

S0897-4756(97)00011-2 CCC: $14.00

when sodium aluminate is added to the synthesis reaction mixture after the mesostructure is formed. We report that the aluminum diffusion can be used to control the spatial distribution of aluminum inside the MCM-41 particles.

Experimental Section

Synthesis Procedure. The procedure for obtaining pure-silica MCM-41 was a hydrothermal procedure that used the effect of salts to improve hydrothermal stability,[6,7] in addition to the pH adjustment during the hydrothermal process to improve the structural order.[8] An aqueous solution of HTACl (25 wt %, Aldrich), a concentrated ammonia solution (28 wt % NH_3), and a sodium silicate solution with the Na/Si ratio of 0.5 (2.4 wt % Na_2O, 9.2 wt % SiO_2, and 88.4 wt % H_2O)[6,7] were well mixed in a polypropylene bottle to obtain HTA−silicate gel with a molar composition of 4 SiO_2:1 HTACl:1 Na_2O:0.15 $(NH_4)_2O$:200 H_2O at room temperature. After the gel was stirred for 1 h, the polypropylene bottle containing the mixture was heated to 370 K in an oven for 1 day (the first heating period). The cap of the bottle was loosened repeatedly to relieve ammonia pressure while temperature was increasing. After the bottle was cooled to room temperature, the pH of the reaction mixture was decreased to 10.2 by dropwise addition of 30 wt % acetic acid with vigorous stirring. The bottle was heated again to 370 K for 1 day (the second heating period) and cooled to room temperature. Subsequently, 8 mol of ethylenediaminetraacetic acid tetrasodium salt ($EDTANa_4$) or 3 mol of NaCl/HTA was added to the reaction mixture in the bottle. The bottle was heated again for 1 day at 370 K (the third heating period). The procedure for the pH adjustment to 10.2 and subsequent heating for 1 day was repeated twice more. Then, the precipitated product was filtered, washed with doubly distilled water and heated for 12 h in a drying oven at 370 K. The dried product was calcined in O_2 flow while the temperature was increased from room temperature to 813 K over 10 h and maintained there for 10 h.

Aluminum-containing MCM-41 (AlMCM-41) samples were obtained by adding 5 wt % aqueous solutions of sodium aluminate (Strem, 99% on metal basis) dropwise to reaction mixtures with vigorous mixing. The reaction mixtures were stirred 30 min more after finishing the addition. The amounts of the aluminate solutions were varied so that the Si/Al ratios for the synthesis mixtures ranged from 2.5 to ∞. The times to add the aluminate solutions were also varied to investigate the effect of the order of mixing the reactants. When the sodium aluminate solutions were added before the first heating period, the remainder of the synthesis procedures was the same as described above. An additional heating period of 2 days or more was given subsequently for Al diffusion when the aluminate solutions were added after the first heating period.

Selective Supporting of Pt Clusters inside Al-Containing Domain of MCM-41 Particles. The procedure to support Pt clusters was the ion exchange of 2 H^+ in AlMCM-41 with $Pt(NH_3)_4^{2+}$.[9] To perform the ion exchange, the AlMCM-41 samples (0.3−3 μm particle size, irregularly shaped) were slurried for 1 h at room temperature in a 1.05×10^{-3} M aqueous solution of $Pt(NH_3)_4(NO_3)_2$ (Aldrich, 100 mL g^{-1}) which contained Pt corresponding to 2 wt % of the resultant Pt/AlMCM-41 samples. The Pt/AlMCM-41 samples were then filtered, washed with doubly distilled water, and dried in a vacuum oven at room temperature. The ion-exchanged platinum species on the AlMCM-41 was activated by heating to 593 K in O_2 flow. The Pt species was converted to Pt clusters by subsequent reduction with H_2 flow at 573 K. Details of the experimental conditions were the same as described previously to obtain 1.0-nm Pt clusters supported on AlMCM-41.[9]

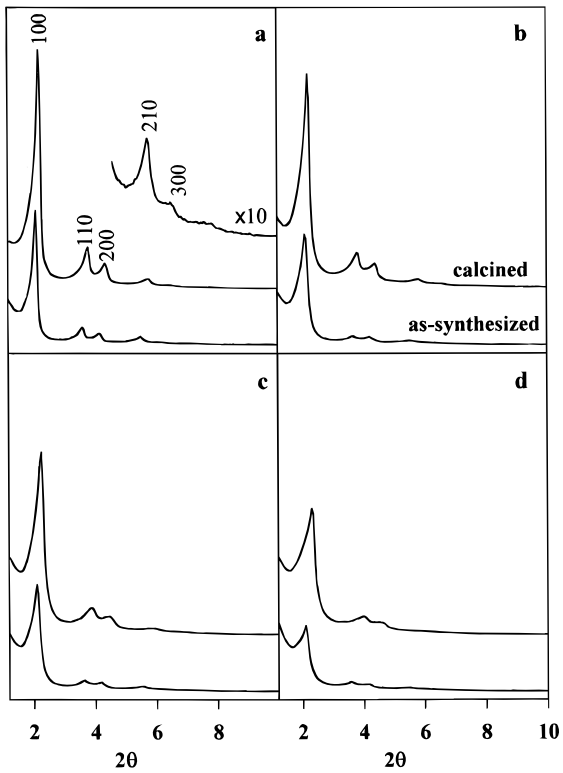

Figure 1. XRD patterns for pure-silica MCM-41 and AlMCM-41: (a) Si/Al = ∞, (b) 30, (c) 15, and (d) 7. Sodium aluminate solution was used as the aluminum source.[6] The sodium aluminate was added to the synthesis mixture 1 h after completing the addition of sodium silicate solution into HTACl solution.

Characterization. Elemental analyses for Si/Al ratios and the Pt content were performed with inductively coupled plasma (ICP) emission spectroscopy (Shimadzu, ICPS-1000III). All AlMCM-41 samples obtained in the present work had the same aluminum content as the Si/Al ratios given with reactants for the synthesis. XRD patterns were obtained with a Cu Kα X-ray source using a Rigaku D/MAX-III (3 kW) instrument.

Magic angle spinning (MAS) ^{27}Al NMR spectra were obtained at 296 K with a Bruker AM 300 instrument operating at 78.2 MHz. Typically, the NMR spectra were obtained using radio frequency pulses for 1.8 μs with 3.0 s recycle delays. The 1.8-μs length corresponded to a 30° pulse for a γ-alumina sample under the same measurement conditions. The effect of the pulse length due to quadrupolar relaxation was also investigated with various pulses in the range 1−5 μs. Samples were spun at 3.5 kHz. ^{129}Xe NMR spectra were collected at 296 K with the same NMR instrument, as described previously.[7,9]

Transmission electron microscopic images were obtained with a Phillips CM20 electron microscope operating at 100 keV. For the TEM experiment, the suspension of the sample powder in ethanol was dropped onto a microporous carbon grid and allowed to dry.

Results

A set of samples with various Si/Al ratios was obtained following the same hydrothermal procedure used for the synthesis of pure-silica MCM-41, except that sodium aluminate solutions were added to the hydrothermal reaction mixture at room temperature 1 h after completing the addition of sodium silicate solution into surfactant solution. Figure 1 shows XRD patterns for the samples, which were measured under the same experimental conditions and displayed on the

(6) Ryoo, R.; Kim, J. M. *J. Chem. Soc., Chem. Commun.* **1995**, 711.
(7) Kim, J. M.; Kwak, J. H.; Jun, S.; Ryoo, R., *J. Phys. Chem.* **1995**, *99*, 16742.
(8) Ryoo, R.; Jun, S. *J. Phys. Chem. B* **1997**, *101*, 317.
(9) Ryoo, R.; Ko, C. H.; Kim, J. M.; Howe, R. *Catal. Lett.* **1996**, *37*, 29.

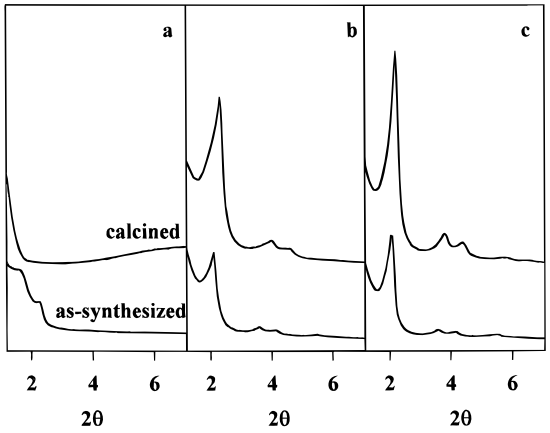

Figure 2. XRD patterns for AlMCM-41 samples with Si/Al = 7: sodium aluminate solution was added (a) into HTACl solution before mixing with sodium silicate solution, (b) 1 h after completing the addition of sodium silicate solution into HTACl solution, and (c) at room temperature following the third heating period (described in the Experimental Section).

same scale. The XRD patterns show systematic decreases in the peak intensity and resolution as the Si/Al ratios decreased. Thus, the structural order was progressively lost with increasing amounts of incorporated aluminum.

Another set of AlMCM-41 samples was also obtained by the same hydrothermal procedure. The same amounts of the sodium aluminate solution were used to give Si/Al = 7. However, the addition of the sodium aluminate solution was performed at various steps of the hydrothermal synthesis procedure, respectively. The XRD patterns for the AlMCM-41 samples with Si/Al = 7 are presented in Figure 2. As Figure 2a shows, the resultant sample had a disordered structure when the sodium aluminate solution was combined with the surfactant solution before the mixing with sodium silicate solution. Compared with the result in Figure 2a, the structural order was improved by mixing the surfactant solution with the sodium silicate solution first and delaying the addition of the sodium aluminate solution until the surfactant−silicate gel was stirred for 1 h at room temperature or heated to 370 K (Figures 2b). The structural order was further improved when the sodium aluminate solution was added to the reaction mixture at room temperature following the third heating period (Figure 2c). Thus, the structural order depended remarkably on the order of mixing the reactants.

A third set of AlMCM-41 samples with various Si/Al ratios ranging from 2.5 to ∞ was obtained following the same hydrothermal procedure used for the synthesis of the above first set of samples, except for the time for the addition of the sodium aluminate solution. The addition of the sodium aluminate solutions for the present set of samples was carried out at room temperature following the third heating step, instead of making the addition before the first heating. The XRD patterns obtained for the present set of samples are presented in Figure 3. The XRD patterns show no distinct changes compared with pure-silica MCM-41 until the Si/Al ratios decreased to 15. Although the XRD patterns began to show the loss of structural disorder as the Si/Al ratios decreased to below 15, the changes were much smaller than those in Figure 1. Figure 4 shows MAS ^{27}Al NMR spectra obtained for the third set of AlMCM-41 samples,

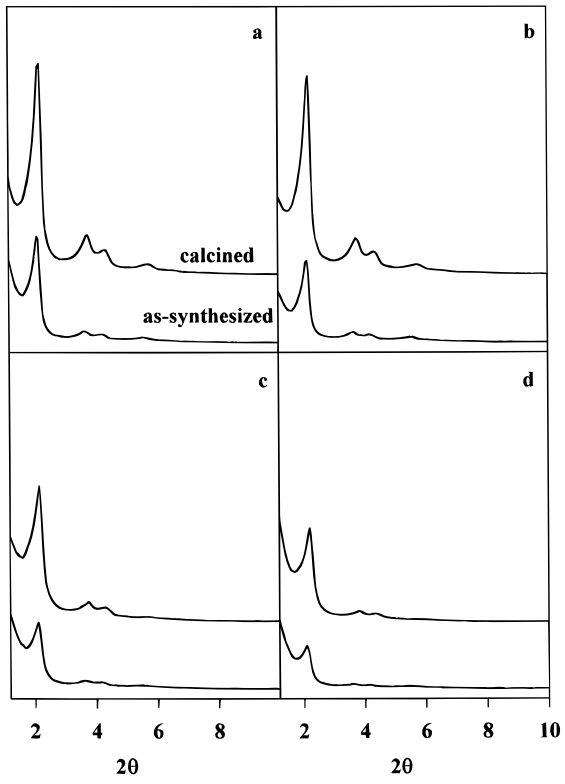

Figure 3. XRD patterns for AlMCM-41 samples displayed against Si/Al ratios: (a) Si/Al = 30, (b) 15, (c) 5, and (d) 2.5. Sodium aluminate solution was added at room temperature following the third heating period (described in the Experimental Section), that is, after completing the formation of surfactant-silicate mesostructures.

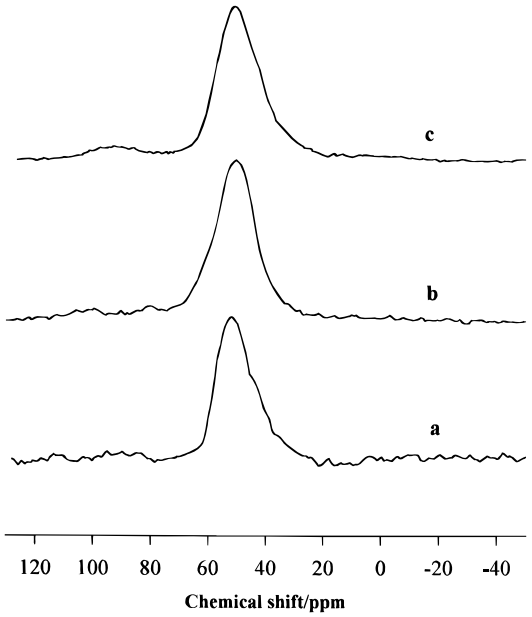

Figure 4. MAS ^{27}Al NMR spectra for AlMCM-41 samples displayed against Si/Al ratios: (a) Si/Al = 30, (b) 15, (c) 5. Samples were obtained by the addition of sodium aluminate solutions after completing the formation of the surfactant-silicate mesostructures as in Figure 3.

which were measured using a pulse for 1.8 μs. The NMR measurement was repeated using vaious pulse lengths between 1 and 5 μs. However, all the NMR spectra consisted of only a single peak with a chemical shift of 50 ppm with respect to $Al(H_2O)_6^{3+}$. The chemical shift was consistent with the aluminum incorporated

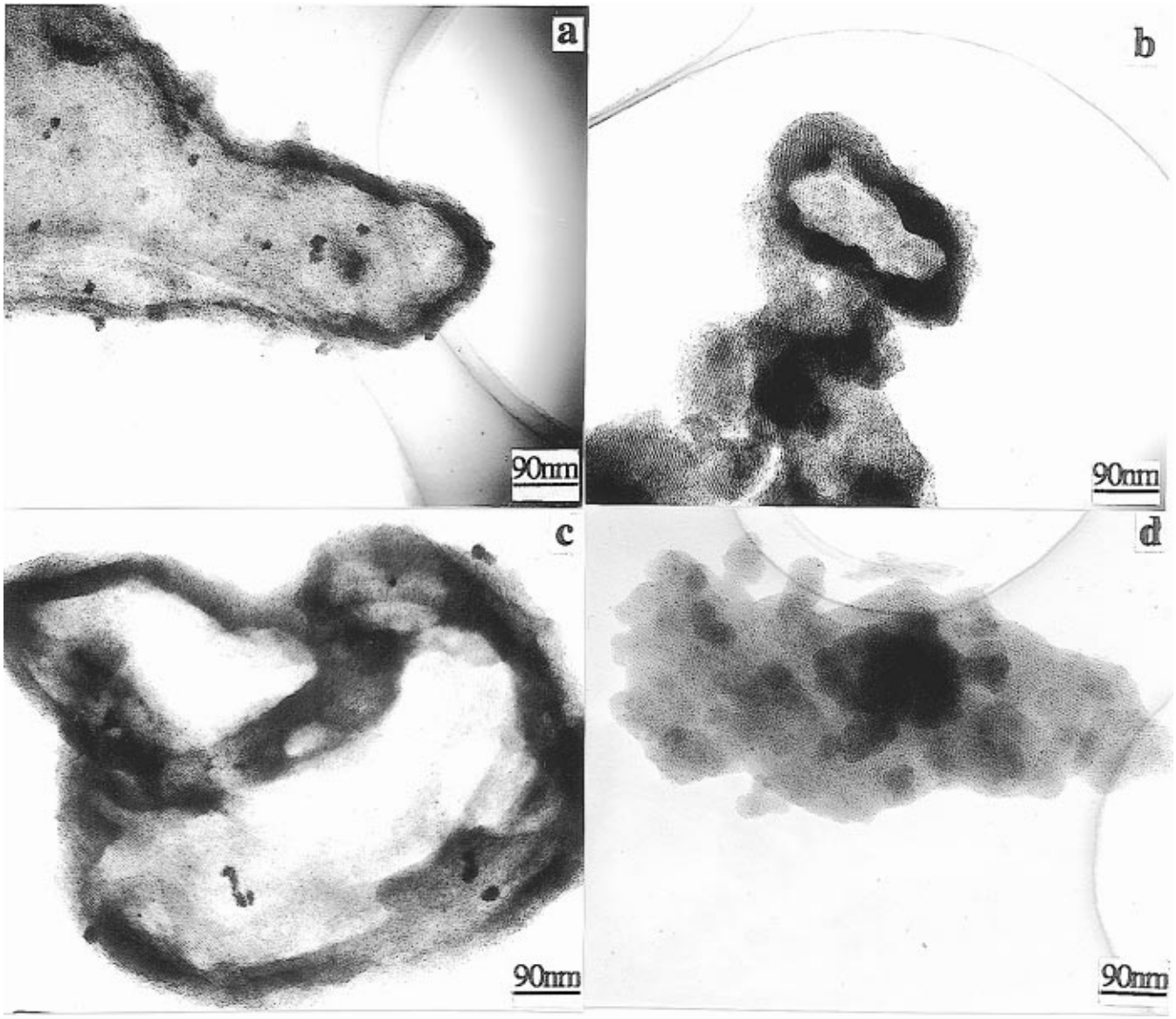

Figure 5. TEM images of AlMCM-41 particles obtained after supporting Pt clusters by ion exchange with $Pt(NH_3)_4^{2+}$. Aluminum source (sodium aluminate solutions) was added after completing formation of the surfactant−silicate mesostructure as in Figure 3. Dark outer regions in the TEM images are due to the loading of Pt clusters, selectively, within Al-containing region of the AlMCM-41 particles. The thickness of the dark regions indicates that the aluminum diffusion was affected by not only Si/Al ratios: (a-c) Si/Al = 30 and (d) Si/Al = 10, but also the heating periods following the addition of the aluminum source: (a) 2 d (b, d) 7 d and (c) 4 weeks.

in the silicate framework with a tetrahedral coordination. No aluminum NMR signal was obtained for the octahedral coordination.

Figure 5 shows TEM images for various AlMCM-41 samples obtained after supporting platinum clusters. Figure 5a was obtained from an AlMCM-41 (Si/Al = 30) sample, for which the aluminum source was added after the third heating step, and subsequently the aluminum diffusion was allowed for 2 days at 370 K. The TEM image of the sample indicates that the Pt clusters, and therefore the tetrahedral aluminum sites, are located within the outer dark region inside the sample particles. Figure 5b was also obtained for the same Si/Al ratio of 30, but the aluminum source for this sample was allowed to diffuse for 7 days. As the TEM images show, their difference in the contact time caused a distinct increase in the thickness of the aluminum-containing region. Figure 5c shows that the aluminum-containing region diffused toward the center of the AlMCM-41 particles as the diffusion time increased to four weeks, compared with Figure 5a,b. Figure 5d was obtained for Si/Al = 10 with the diffusion time of 7 days. The TEM image with Si/Al = 10 shows a homogeneous distribution of platinum clusters, which indicates that the aluminum diffused into the center of the particle. In contrast to the heterogeneous distribution of aluminum shown in Figure 5a−c, TEM images indicating a homogeneous distribution of aluminum were obtained even for samples with Si/Al ratios as high as 30 when the aluminum source was added before the first heating of the synthesis mixture. No separate, dense aluminosilicate domains similar to a report by Kloetstra et al.[10] were found in the TEM images. All the samples gave the specific surface areas in the range of 900 ± 100 m^2 g^{-1} obtained by the BET method.

(10) Kloetstra, K. R.; Zandbergen, H. W.; van Bekkum, H. *Catal. Lett.* **1995**, *33*, 157.

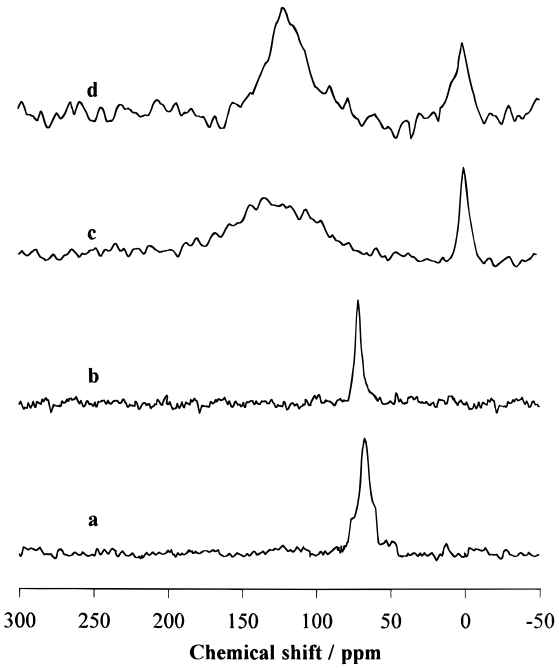

Figure 6. ^{129}Xe NMR spectra obtained from calcined MCM-41 samples at 53.3 kPa of xenon pressure at 296 K: (a) AlMCM-41 with Si/Al = 30, (b) AlMCM-41 with Si/Al = 10, (c) AlMCM-41 with Si/Al = 30 after supporting 2 wt % Pt clusters, and (d) AlMCM-41 with Si/Al = 10 after supporting 2 wt % Pt clusters. The NMR line in (c) is broader than (d), due to the heterogeneous distribution of Pt clusters inside the AlMCM-41 particles.

Figure 6 shows ^{129}Xe NMR spectra for AlMCM-41 samples with Si/Al ratios of 30 and 10. The samples were prepared with the addition of sodium aluminate solutions after the third heating step and allowed the aluminum diffusion to occur for 7 days. All the xenon NMR spectra were obtained under the same experimental conditions of 53.3 kPa at 296 K. The two samples before supporting Pt clusters showed an NMR peak with almost the same line shape and chemical shift of 65 ppm with respect to xenon gas at infinite dilution. After the Pt clusters were supported, both samples showed similar increases in the chemical shift to about 120−130 ppm. However, the NMR line width for the sample with Si/Al = 30 became very broad after the platinum incorporation, compared with the sample with Si/Al = 10.

Discussion

A major effect due to the aluminum incorporation in MCM-41 is the loss of the structural order. The structural order decreases progressively as the level of the aluminum incorporation increases, as shown in Figure 1, if the same aluminum source is used according to the same order of mixing the reactants. Figure 2 shows that the structural order is very much influenced by the order of mixing the reactants. Moreover, previous work on the aluminum incorporation using various aluminum sources has indicated that the structural order is also influenced by the nature of the aluminum sources.[5] The cause of the effect by the nature of the aluminum sources is unknown and beyond the scope of our discussion. Consequently, our discussion here is limited to the incorporation of aluminum using sodium aluminate.

Considering the structural disorder due to the aluminum incorporation in MCM-41, it is useful to correlate the addition time of the aluminum source with the formation of the surfactant−silicate mesostructures. For this purpose, we have analyzed the structure of the mesostructures obtained at various steps during the hydrothermal synthesis procedure. First, we separated a solid or gellike material from the reaction mixture using a centrifuge 1 h after completing the addition of the sodium silicate solution into the surfactant solution. The material thus obtained gave an XRD pattern characteristic of the MCM-41 structure. The appearance of the MCM-41-like XRD pattern indicates that the surfactant−silicate mesophase begins to form before the heating of the reaction mixture to 370 K, similar to the room-temperature syntheses of MCM-41 reported previously.[11,12]

Although the formation of the surfactant−silicate mesophase takes place at room temperature under the present synthesis condition, the mesostructure formed at room temperature has a relatively low X-ray diffraction intensity and resolution. While one or two XRD peaks are poorly resolved in the XRD pattern for the mesostructure obtained at room temperature, the mesostructure obtained after heating the reaction mixture for 1 day at 370 K has four XRD peaks with high resolution and intensity. However, the mesostructure thus obtained has a large number of excess silanol groups, due to the low degree of silicate cross-linking in the framework. The excess silanol groups are forced to condense during calcination, leading to lattice contraction as much as 25%.[5a,6] The structural order is also severely lost during the lattice contraction. The lattice contraction and loss of the structural order upon calcination can be prevented by repeating the pH adjustment to 10.2 and subsequent heating to 370 K alternatively after the first heating. Five well-resolved XRD peaks similar to Figure 1a can be obtained from pure-silica MCM-41 samples obtained after alternating the pH adjustment and heating three subsequent times. The XRD line width changes very little during subsequent calcination. The lattice contraction occurs less than 3% during the calcination. The pore-size distribution for the calcined sample shows a peak with the width less than 0.3 nm at half the full height, in the mesopore range.[8] These effects resulting from the pH adjustment during the hydrothermal synthesis can be attributed to shifts in the reaction equilibrium toward the silicate condensation while the framework is supported by the surfactant.[6]

The purpose of the addition of NaCl and $EDTANa_4$ in the present synthesis procedure is to improve hydrothermal stability of calcined MCM-41 products.[13] The effect of using various salts such as NaCl and $EDTANa_4$ for the improvement of hydrothermal stability of MCM-41 has been discovered very recently by Ryoo and Jun.[8] They have reported that the hydrothermal stability increased remarkably as the amount of salts was increased to a certain level. However, excess salts led not only to a decrease in the hydrothermal stability but

(11) Stucky, G. D.; Monnier, A.; Schüth, F.; Huo, Q.; Margolese, D.; Kumar, D.; Krishnamurty, M.; Petroff, P.; Firouzi, A.; Janicke, M.; Chmelka, B. F. *Mol. Cryst. Liq. Cryst.* **1994**, *240*, 187.
(12) Edler, K. J.; White, J. W. *J. Chem. Soc., Chem. Commun.* **1995**, 155.
(13) Kim, J. M.; Ryoo, R. *Bull. Korean Chem. Soc.* **1996**, *17*, 66.

also to a loss of the structural order. For example, the structure of the calcined MCM-41 samples obtained without the salts was lost almost completely during heating in water for 12 h at 343 K, although the XRD pattern before the heating in water was similar to that in Figure 1a. When 3 mol of NaCl were added per HTACl during the hydrothermal synthesis, the resultant materials after calcination showed no sign of the structural disintegration in the XRD pattern even after 12 h in boiling water. When 6 mol of NaCl were used, the hydrothermal stability decreased compared with that found using 3 mol of NaCl. The effect of salts improving hydrothermal stability is also effective for the synthesis of AlMCM-41. However, the exact cause of the effects of salts has not been clarified yet.

As discussed above, the surfactant−silicate mesostructure for MCM-41 begins to form at room temperature when the surfactant is mixed with sodium silicate solution. However, the mesostructure obtained at room temperature has low structural order. It is reported that the product yield based on the silica recovery was 65% after the first heating for 1 day at 370 K, under an experimental condition similar to the present synthesis. The OH/Si ratio obtained by MAS ^{29}Si NMR was about 0.6.[6] The product yield increased to about 90% at the second heating step, and the silanol group content decreased to 0.3 OH/Si. The product yield and the silanol group content did not change significantly afterward. The report indicates that the formation of the mesostructure is completed during the second heating period under the present synthesis condition. Therefore, the effects of the order of mixing the reactants shown in Figure 2 can be discussed with a correlation between the addition time of the aluminum source and the formation of the surfactant−silicate mesostructure. Evidently, the sodium aluminate solution in the case of Figure 2a was mixed with the surfactant solution before the mesostructure began to form. The resultant broad XRD pattern is consistent with results obtained by others with the addition of aluminum sources before mixing surfactants with silica sources.[10,14,15] The broad XRD pattern is similar to the XRD patterns for the disordered mesoporous structures which have been suggested to be hexagonal-like,[16] wormlike,[17] random,[18] and noodle-like[10] arrangements of mesoporous tubes, or the three-dimensional disordered network of mesoporous channels which has been proved using TEM images of the Pt wires incorporated inside the channels.[19] On the other hand, the addition of the aluminum source in the case of Figure 2b was delayed until the formation of the surfactant−silicate mesostructure proceeded considerably. In the case of Figure 2c, the addition of the aluminum source was further delayed until the formation of the mesostructure was completed. From these results, it is reasonable that the structural order of the resulting AlMCM-41 samples was improved by delaying the addition of the aluminum source until the formation of the surfactant−MCM-41 mesostructure was completed.

The dependence of the XRD line widths on the order of mixing the reactants, shown in Figures 2a−c, is very similar to the effect of salts on the structural order reported by Ryoo and Jun.[8] They have reported that the addition of various salts such as NaCl and $EDTANa_4$ into surfactant solutions before mixing with the sodium silicate solution led to the formation of a disordered mesostructure, while the addition after completing the formation of the surfactant−silicate mesostructure for MCM-41 resulted in the preparation of well-ordered MCM-41 materials. The present effects due to the addition of the aluminum source may be explained using the effect on Gibbs free energy,[20] similar to the effect of salts.

According to the elemental analysis, the total amount of aluminum added to the synthesis mixture was found to be incorporated in the resultant AlMCM-41 samples. Thus, it was possible to achieve the aluminum incorporation by adding the aluminum source at various times during the formation of the surfactant−silicate mesostructures. Furthermore, all the as-synthesized and calcined AlMCM-41 samples showed only the MAS ^{27}Al NMR signal coming from the tetrahedral coordination. No octahedral aluminum NMR signals were found irrespective of the Si/Al ratios. Although the MAS ^{27}Al NMR signal intensity increased consistently with the aluminum content, the NMR signal intensity may not be used for the quantitative determination. The proportionality between the area under MAS ^{27}Al NMR peak and aluminum content may fail if the line width due to the quadrupolar spin relaxation is sufficiently large to make the species not observable within the experimental limitations of the spectrometer. A small octahedral component may be invisible if the nutation flip angle for ^{27}Al nuclear spin excitation is nonselective to the central ($^1/_2$,$-^1/_2$) transition. The effect of quadrupolar spin relaxation has been investigated for the present samples using various pulse lengths in the range 1−5 μs. However, the result showed no NMR signal due to the octahedral component. The result for the present samples may be compared with ^{27}Al NMR spectra for MCM-41 samples which were prepared to contain nonframework aluminum by the impregnation of an aqueous solution of $AlCl_3$. The MCM-41 samples containing nonframework aluminum showed two NMR peaks due to not only the tetrahedrally coordinated aluminum but also octahedrally coordinated aluminum. Relative peak intensity between the two NMR signals for the sample containing framework aluminum indeed showed a large dependence on the pulse length under the measurement conditions.

Kim et al. reported that AlMCM-41 has very high cation-exchange capacities compared with pure-silica MCM-41, due to tetrahedral aluminum similar to the ion exchange of zeolites.[7] The ion-exchange property of AlMCM-41 was used later by Ryoo et al. to support Pt clusters for catalysis.[9] Their procedure to obtain small Pt clusters with 1-nm diameter after the ion exchange of $Pt(NH_3)_4^{2+}$ was the same procedure that was used in the present work, using calcination and

(14) Luan, Z.; Cheng, C.-F.; He, H.; Klinowski, J. *J. Phys. Chem.* **1995**, *99*, 10590.
(15) Borade, R. B.; Clearfield, A. *Catal. Lett.* **1995**, *31*, 267.
(16) Chen, C.-Y.; Xiao, S.-Q.; Davis, M. E. *Microporous Mater.* **1995**, *4*, 1.
(17) Bagshaw, S. A.; Prouzet, E.; Pinnavaia, T. J. *Science* **1995**, *269*, 1242.
(18) Guo, C. J. In *Zeolites: A Refined Tool for Designing Catalytic Sites*; Bonneviot, L., Kaliaguine, S., Eds.; Elsevier: Amsterdam, 1995; *Studies in Surface Science and Catalysis*; Vol. 97, p 165.
(19) (a) Ryoo, R.; Kim, J. M.; Ko, C. H.; Shin, C. H. *J. Phys. Chem.* **1996**, *100*, 17718. (b) Ko, C. H.; Ryoo, R. *Chem. Commun.* **1996**, 2467.

(20) "The chemical potential" in ref 8 should be corrected to "Gibbs free energy".

reduction treatments. The small Pt clusters prepared by the procedure are located inside the mesoporous channels of the AlMCM-41 particles. No migration of the Pt species occurs from the channels to the external surface of the AlMCM-41 particles during the preparation of the clusters. Therefore, the dark image due to Pt clusters in Figure 5 corresponds to the domain containing the tetrahedral aluminum, where the Pt cluster was supported by the ion exchange of $Pt(NH_3)_4^{2+}$. The heterogeneous images in Figures 5a−c show that the framework aluminum was heterogeneously distributed inside the AlMCM-41 particles. On the other hand, Figure 5d shows that the aluminum was homogeneously distributed. The TEM images are consistent with the ^{129}Xe NMR spectra shown in Figure 6. The NMR line shown in Figure 6c is broad, due to the sample heterogeneity, compared with Figure 6d. Similar effects of the heterogeneous line broadening in ^{129}Xe NMR spectroscopy have been reported previously with zeolite mixtures[21] and poorly ordered MCM-41.[6] Therefore, it is clear that the aluminum was incorporated by the diffusion into MCM-41 particles from the reaction mixture after the formation of the surfactant−silicate mesostructures. The diffusion progressed toward the center of the particles as the Si/Al ratios decreased and the diffusion time increased. Interesting comparisons may be made between the TEM imaging results and quantitative information from energy-dispersive X-ray emission analysis.

Conclusions. Results reported by the present work indicate that aluminum can be incorporated into the siliceous framework of MCM-41 by adding sodium aluminate into the synthesis reaction mixture before, during, or after completing the formation of the surfactant−silicate mesostructure. If the aluminum source is added after completing the formation of the mesostructure, the aluminum incorporation occurs through slow diffusion into the mesostructure over many days. The aluminum incorporation by diffusion produces AlMCM-41 samples exhibiting high structural order, compared with the mixing of the sodium aluminate before the formation of the mesostructure. The distribution of aluminum can be visualized by transmission electroscopic images obtained after supporting Pt clusters selectively inside the aluminum-containing region by the ion exchange of $Pt(NH_3)_4^{2+}$. The information on the aluminum distribution obtained by the imaging technique can be useful for rational design of catalytic materials based on MCM-41. In addition, the method incorporating aluminum after completing the formation of surfactant−silicate mesostructure may be useful for aluminum incorporation to other mesoporous silicate materials such as MCM-48,[1] and SBA-1,2,3,[22] MSU-1,[17] KIT-1,[19] and so on, found more recently.

Acknowledgment. R.R. is grateful for financial support from the Australian Research Council for sabbatical leave from KAIST at UNSW to perform the present research.

CM9700110

(21) Ryoo, R.; Pak, C.; Chmelka, B. F. *Zeolites* **1990**, *10*, 790.

(22) Huo, Q.; Leon, R.; Petroff, P. M.; Stucky, G. D. *Science* **1995**, *268*, 1324.